

Double boxes and double dimers

Tatyana Benko^{*1} and Benjamin Young⁺¹

¹*Department of Mathematics, University of Oregon, Eugene, OR, USA*

Abstract. We give a combinatorial proof of a result in rank 2 Donaldson–Thomas theory, which states that the generating function for certain plane-partition-like objects, called double-box configurations, is equal to a product of MacMahon’s generating function for (boxed) plane partitions. In our proof, we first give the correspondence between double-box configurations and double-dimer configurations on the hexagon lattice with a particular tripartite node pairing. Using this correspondence, we apply graphical condensation and double-dimer condensation to prove the result.

Keywords: Plane partitions, double-box configurations, dimer model, Donaldson–Thomas theory, condensation

1 Introduction

In this extended abstract, we enumerate certain plane-partition-like objects called *double-box configurations*. These objects were introduced by Gholampour, Kool and Young [2] for the purpose of computing the rank 2 Donaldson–Thomas (DT) invariants of a Calabi–Yau threefold. We define double-box configurations in [Definition 2](#), as well as their generating function, $Z_{DBC}^{a,b,c}(q)$, in [Equation 2.2](#), and we give a combinatorial proof of the following geometrically motivated theorem:

Theorem 1. *Let $a, b, c \in \mathbb{N}$, then*

$$Z_{DBC}^{a,b,c}(q) = M(q)^2 M_{a,b,c}(q) \tag{1.1}$$

where $Z_{DBC}^{a,b,c}(q)$ denotes the generating function for double-box configurations, and

$$M(q) = \prod_{i=1}^{\infty} \frac{1}{(1 - q^i)^i}$$

is MacMahon’s generating function for plane partitions, and

^{*}tbenko@uoregon.edu. Tatyana Benko was partially funded by NSF grant DMS-2039316.

⁺bjy@uoregon.edu

$$M_{a,b,c}(q) = \prod_{s=1}^a \prod_{t=1}^b \prod_{r=1}^c \frac{1 - q^{s+t+r-1}}{1 - q^{s+t+r-2}}$$

is MacMahon's generating function for boxed $a \times b \times c$ plane partitions.

Note that this formula already has a geometric proof [1]. In this paper, we outline our combinatorial proof of this formula, which surprisingly uses the tripartite double-dimer model of Kenyon and Wilson [5]. We follow the general strategy of [4], where the tripartite double-dimer model also appears (though for apparently completely different reasons). Our proof consists of two main components. First, we give a correspondence between double-box configurations and tripartite double-dimer configurations on the hexagon lattice; this correspondence is many-to-one, yet still weight preserving. Next, we use a quadratic recurrence called condensation to prove our main result. We show that to the left hand side of Equation 1.1, $Z_{DBC}^{a,b,c}(q)$, we may apply a result by Jenne [3], which states that under certain conditions the generating function for tripartite double-dimer configurations satisfies a recurrence relation related to the Desnanot–Jacobi identity from linear algebra. Then, using Kuo condensation [6] (also related to the Desnanot–Jacobi identity), we show that $M(q)^2 M_{a,b,c}(q)$ satisfies the same recurrence relation. Finally, we show that both sides of Equation 1.1 satisfy the same initial conditions.

The full version of this abstract will appear in a longer paper; proofs and some details have been omitted here due to space constraints.

2 Definitions

A *plane partition* is a two-dimensional array of nonnegative integers $\pi_{i,j}$ for $i, j \geq 0$, with $\pi_{i,j+1} \geq \pi_{i,j}$ and $\pi_{i+1,j} \geq \pi_{i,j}$ for all i, j , with finitely many $\pi_{i,j}$ being nonzero. We can visualize a plane partition π as a stack of boxes in the corner of a room, with the number of boxes in each stack given by the entries of π . A *dimer configuration* (also called a *perfect matching*) on a graph $G = (V, E)$ is a collection of edges $E' \subseteq E$ such that every vertex in V is covered exactly once. There is a bijection between plane partitions and dimer configurations on the hexagon graph, sometimes referred to as the *folklore bijection* (see Figure 1). The stacks of boxes representing a plane partition π can be viewed as a lozenge tiling of a hexagonal region of triangles, corresponding to the visible faces of the boxes and the tiles on the walls and floor of the room. Note that the triangular lattice is dual to the hexagon lattice. Moreover, each lozenge is made of two equilateral triangles that share an edge. If we join the centers of these two triangles with the corresponding dual edge, and do this for all tiles in the tiling, we get a perfect matching on the hexagon graph.

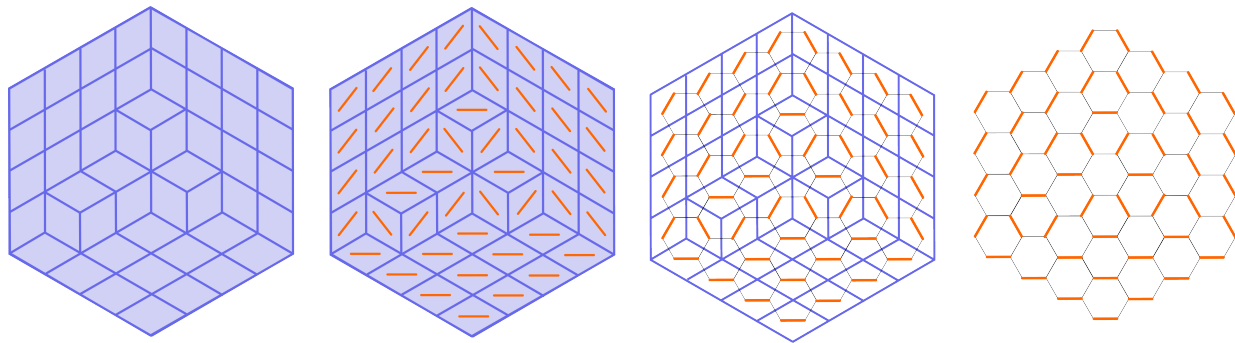


Figure 1: Folklore bijection between plane partitions (left-most) and dimer configurations on the hexagon graph (right-most)

Overlaying two perfect matchings of a graph $G = (V, E)$ gives a *double-dimer configuration*, which consists of doubled edges and loops. If in addition we have defined a set of nodes $N \subset V$, that is, a special set of vertices, then the double-dimer configuration on $G = (V, E)$ with node set N is a multiset of edges of E such that each vertex in $V \setminus N$ is covered exactly twice, and each node in N is covered exactly once. In this case, the double-dimer configuration consists of doubled edges, loops, and paths between the nodes in N (see Figure 2).

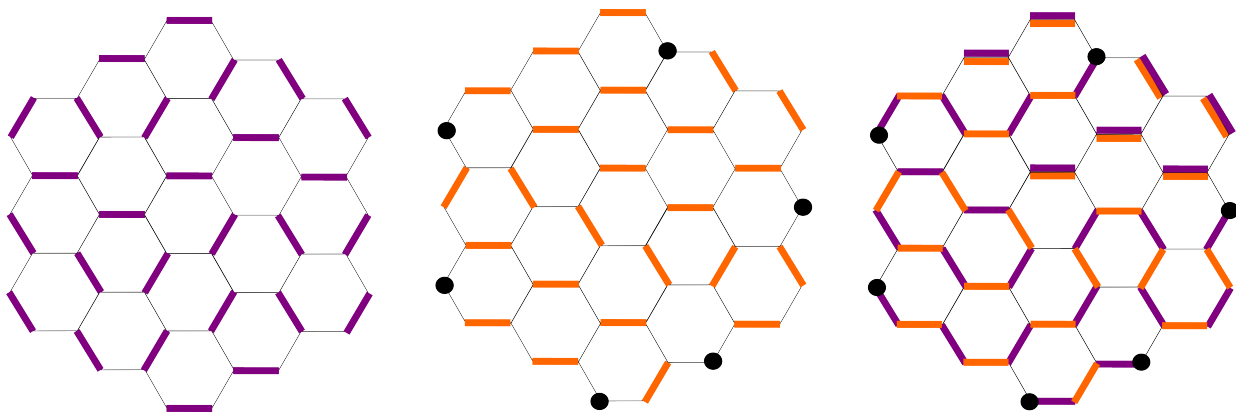


Figure 2: Double-dimer configuration with nodes on the hexagon graph (right-most) from two single-dimer configurations, one on the hexagon graph (left-most) and one on the hexagon graph minus the defined nodes (middle)

2.1 Double-box configurations

In this section we define the double-box configurations [2], and provide some examples. Throughout this section we let $a, b, c \in \mathbb{N}$ be fixed. We identify the point $(i, j, k) \in \mathbb{Z}^3$

with the unit cube

$$[i, i+1] \times [j, j+1] \times [k, k+1] \in \mathbb{R}^3.$$

We refer to this unit cube as the box (i, j, k) . We consider plane partitions as stacks of unit cubes (i.e. boxes) placed in \mathbb{R}^3 . A plane partition π is said to be based at (l, m, n) in \mathbb{R}^3 if the bottommost box in the stack of boxes corresponding to the entry in the first row and column of π is the box (l, m, n) . In other words, the back corner of the room where the boxes are stacked is placed at (l, m, n) .

Consider triples of plane partitions $\eta = (\eta_1, \eta_2, \eta_3)$ such that η_1 is based at $(0, b, c)$, η_2 is based at $(a, 0, c)$, and η_3 is based at $(a, b, 0)$ in \mathbb{R}^3 (see Figure 3). We say that a box (i, j, k) is in the *intersection space* if $i \geq a$, $j \geq b$, and $k \geq c$. We denote all the boxes in the intersection space by η_{int} .

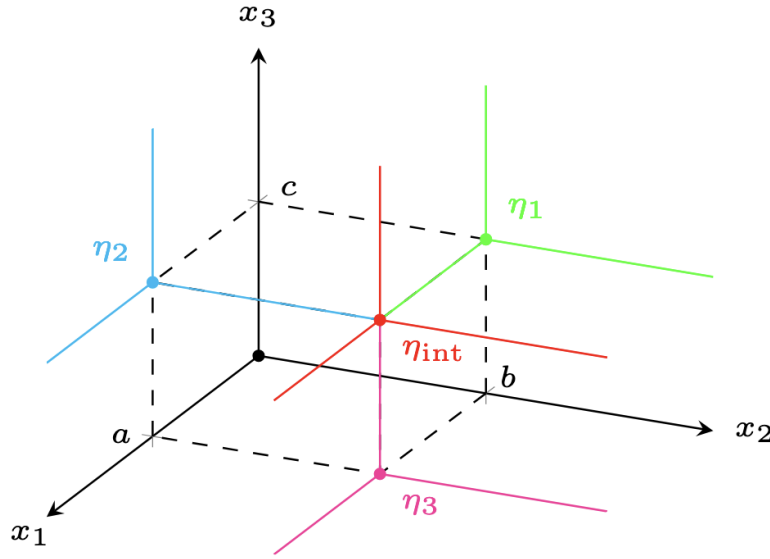


Figure 3: Basepoints of plane partitions η_1, η_2, η_3 in \mathbb{R}^3

We define different types of boxes based on the number of plane partitions they are contained in as:

Definition 1. We say that a box $(i, j, k) \in \eta = (\eta_1, \eta_2, \eta_3)$ is:

- a *type III box* if $(i, j, k) \in \eta_1, \eta_2, \eta_3$ (triple intersection boxes)
- a *type II box* if $(i, j, k) \in \eta_m, \eta_n$ and $(i, j, k) \notin \eta_l$ for $\{m, n, l\} = \{1, 2, 3\}$ (double intersection boxes)

- a type I box if $(i, j, k) \in \eta_m$ and $(i, j, k) \notin \eta_n, \eta_l$ for $\{m, n, l\} = \{1, 2, 3\}$ (boxes in only one of the plane partitions)

Let η_{in} denote the set of type III boxes, and let η_{out} denote the set of type II boxes. Note that $\eta_{\text{in}} \cup \eta_{\text{out}}$ is a plane partition based at (a, b, c) , with $\eta_{\text{in}} \cup \eta_{\text{out}} \subseteq \eta_{\text{int}}$. We want to consider triples of plane partitions $\eta = (\eta_1, \eta_2, \eta_3)$ such that the following Criterion is satisfied:

Criterion 1. $\eta_{\text{int}} = \eta_{\text{in}} \cup \eta_{\text{out}}$,

that is,

$$\eta_{\text{int}} = (\eta_1 \cap \eta_2) \cup (\eta_1 \cap \eta_3) \cup (\eta_2 \cap \eta_3). \quad (2.1)$$

We define an equivalence relation on triples of plane partitions satisfying Criterion 1 as follows. If $\eta = (\eta_1, \eta_2, \eta_3)$ and $\tilde{\eta} = (\tilde{\eta}_1, \tilde{\eta}_2, \tilde{\eta}_3)$, we say that $\eta \sim \tilde{\eta}$ if they have the same multiset of boxes. That is, $\eta \sim \tilde{\eta}$ if:

- $\eta_{\text{in}} = \tilde{\eta}_{\text{in}}$ (type III boxes the same)
- $\eta_{\text{out}} = \tilde{\eta}_{\text{out}}$ (type II boxes the same, regardless of which two partitions they came from)
- η_1 agrees with $\tilde{\eta}_1$ on $[0, a) \times [b, \infty) \times [c, \infty)$
- η_2 agrees with $\tilde{\eta}_2$ on $[a, \infty) \times [0, b) \times [c, \infty)$
- η_3 agrees with $\tilde{\eta}_3$ on $[a, \infty) \times [b, \infty) \times [0, c)$

The last three conditions ensure that all type I boxes, that is, those not in the intersection space by Criterion 1, are the same. We are now ready to define double-box configurations as:

Definition 2. Given $(a, b, c) \in \mathbb{N}^3$, an equivalence class of triples of plane partitions $\eta = (\eta_1, \eta_2, \eta_3)$ satisfying Criterion 1 under the equivalence relation \sim is called a double-box configuration. Note that we often denote such an equivalence class by η , rather than $[\eta]$.

We denote the set of all double-box configurations by $DBC_{a,b,c}$. For each $\eta \in DBC_{a,b,c}$, we define the following:

Definition 3. The weight of a double-box configuration $\eta = (\eta_1, \eta_2, \eta_3)$ is defined as

$$\begin{aligned} |\eta| &= |\eta_1| + |\eta_2| + |\eta_3| - |\eta_{\text{int}}| \\ &= \#\{\text{type I boxes}\} + \#\{\text{type II boxes}\} + 2 \cdot \#\{\text{type III boxes}\}. \end{aligned}$$

Note that this quantity is well-defined on equivalence classes.

Next, we consider elements within the equivalence class of a double-box configuration $[\eta]$. To do this, we first make the following definition:

Definition 4. A box $(i, j, k) \in \eta_{\text{out}}$ is said to be *moveable* if there exists $\hat{\eta} \neq \tilde{\eta} \in [\eta]$ and two indices $m \neq n \in \{1, 2, 3\}$ such that $(i, j, k) \notin \hat{\eta}_m$ and $(i, j, k) \notin \tilde{\eta}_n$.

Triples of plane partitions within an equivalence class (i.e. a double-box configuration), may differ by which two plane partitions a moveable box is contained in. We consider several examples to illustrate this.

Example 1. Let $(a, b, c) = (1, 1, 1)$. Consider $\eta = (\eta_1, \eta_2, \eta_3)$ and $\tilde{\eta} = (\tilde{\eta}_1, \tilde{\eta}_2, \tilde{\eta}_3)$ as defined in Figure 4.

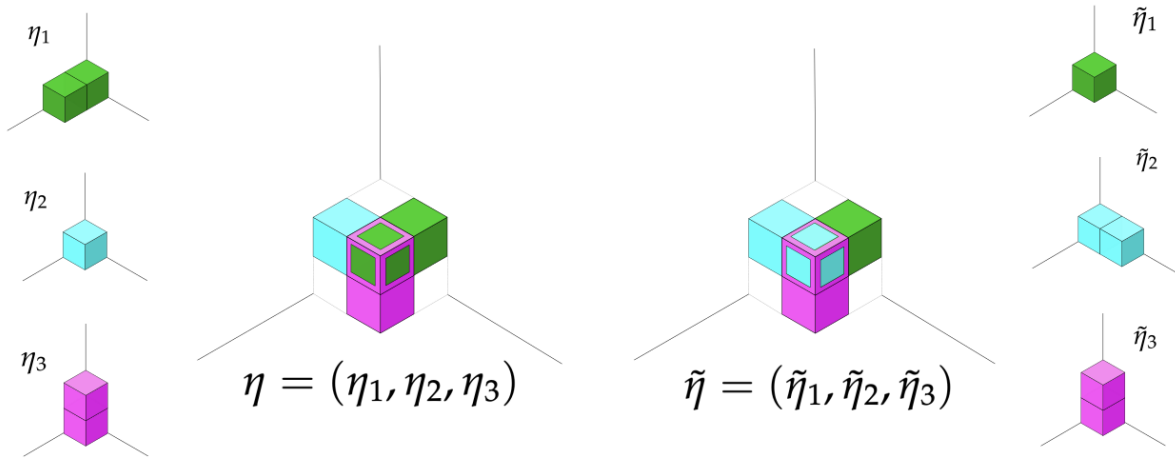


Figure 4: Example of $\eta \neq \tilde{\eta}$ with $[\eta] = [\tilde{\eta}]$.

There is one type II box in this double-box configuration at $(1, 1, 1)$. In η , this box is contained in η_1 and η_3 , and in $\tilde{\eta}$ this box is contained in $\tilde{\eta}_2$ and $\tilde{\eta}_3$. Since η and $\tilde{\eta}$ contain the same multiset of boxes, we have that $[\eta] = [\tilde{\eta}]$, and so the type II box at $(1, 1, 1)$ is a moveable box.

Example 2. Let $(a, b, c) = (1, 1, 1)$, and consider $\eta = (\eta_1, \eta_2, \eta_3)$ as defined in Figure 5.

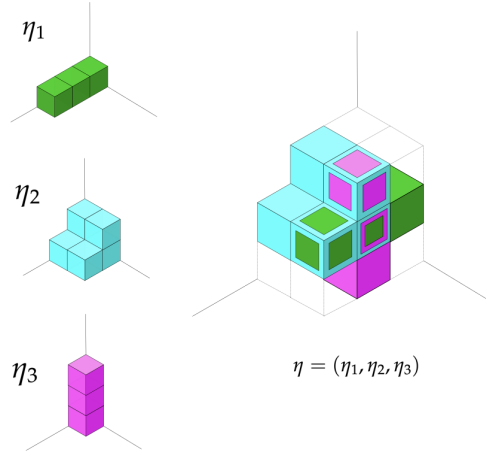


Figure 5: Example of a double-box configuration.

In this example, there is one type III box at $(1, 1, 1)$, and two type II boxes, one at $(2, 1, 1)$ contained in η_1 and η_2 , and one at $(1, 1, 2)$ contained in η_2 and η_3 . Both of these type II boxes are not moveable. The box at $(1, 1, 2)$ cannot be contained in η_1 because $(0, 1, 2) \notin \eta_1$, and the box at $(2, 1, 1)$ cannot be contained in η_3 because $(2, 1, 0) \notin \eta_3$.

To define the generating function for double-box configurations, we first make the following definition:

Definition 5. The contribution of a double-box configuration η is defined as

$$\chi(\eta) = 2^m$$

where m is the number of connected components of moveable boxes in η . Two boxes are in the same connected component if they share a face.

Finally, we define the generating function for double-box configurations as

$$Z_{DBC}^{a,b,c}(q) = \sum_{\eta \in DBC_{a,b,c}} \chi(\eta) q^{|\eta|}, \quad (2.2)$$

where $|\eta|$ is defined in Definition 3, and $\chi(\eta)$ is defined in Definition 5.

2.2 Tripartite double-dimer configurations

In this section we will define the tripartite node pairing of the double-dimer configurations on the hexagon graph. Let $H(n)$ be the hexagon graph of size $n \times n \times n$. That

is, project the points $\{0, \dots, n\}^3 \subset \mathbb{N}^3$ onto the plane $P : \{x + y + z = 0\}$ to obtain the vertices of a hexagon-shaped piece of the triangular lattice; $H(n)$ is the planar dual of this graph, without an external vertex. Choose coordinates (x, y) for P such that a third of the edges are parallel to the x axis - "horizontal" - and the others have slope $\pm\sqrt{3}/2$. For convenience, we will use standard "compass coordinates" to describe directions on this picture - so "North" is the positive y direction, "West" is negative x , and so on (see Figure 6).

Next, let A be the southwest corner of $H(n)$ (that is, the intersection of the lines L_1 and L_2 in Figure 6), let B be the southeast corner (intersection of L_3 and L_4), and let C be the north corner of $H(n)$ (intersection of L_5 and L_6). We define the following sets of nodes, i.e. special vertices, on the boundary of $H(n)$

$$R = \{a \text{ nodes on } L_1 \text{ closest to } A\} \cup \{c \text{ nodes on } L_2 \text{ closest to } A\}$$

$$G = \{c \text{ nodes on } L_3 \text{ closest to } B\} \cup \{b \text{ nodes on } L_4 \text{ closest to } B\}$$

$$B = \{b \text{ nodes on } L_5 \text{ closest to } C\} \cup \{a \text{ nodes on } L_6 \text{ closest to } C\}$$

Note that $|R| = a + c$, $|G| = b + c$, and $|B| = a + b$, satisfy the triangle inequality, and so there is a unique planar *tripartite pairing* of the nodes, we call this pairing $\sigma_{a,b,c}$. The planar tripartite pairing $\sigma_{a,b,c}$ matches the a red nodes on L_1 with the a blue nodes on L_6 , the b blue nodes on L_5 with the b green nodes on L_4 , and the c red nodes on L_2 with the c green nodes on L_3 , so that each node is paired with another node of a different color (see Figure 6).

Let $DDC_n(\sigma_{a,b,c})$ be the set of all double-dimer configurations on $H(n)$ with node set $N = R \cup G \cup B$ and tripartite pairing $\sigma_{a,b,c}$. We define the generating function for elements in $DDC_n(\sigma_{a,b,c})$ as

$$Z_{DDC}^{n,a,b,c}(q) = \frac{1}{w(\pi_0)} \sum_{\pi \in DDC_n(\sigma_{a,b,c})} 2^{\ell(\pi)} w(\pi) \quad (2.3)$$

where $\ell(\pi)$ is the number of closed loops of π , and the configuration $\pi_0 \in DDC_n(\sigma_{a,b,c})$ has minimal weight. The weight of a double-dimer configuration π is given by

$$w(\pi) = \prod_{e \in \pi} w(e)$$

where $w : E \rightarrow \mathbb{Q}[q]$ for an indeterminate q is a weighting on the edge set of $H(n)$ such that the generating function for plane partitions is the same as the one for single-dimer configurations on $H(n)$ up to a constant. With this weighting, the normalized weight of a tripartite double-dimer configuration equals the weight of the corresponding double-box configuration (this correspondence is discussed in Section 3). We also show that

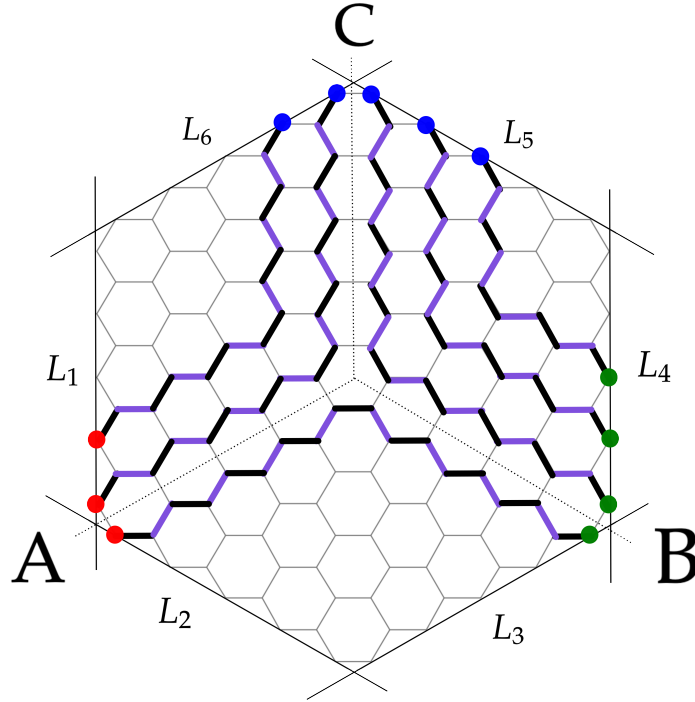


Figure 6: Tripartite node pairing $\sigma_{a,b,c}$ with $a = 2$, $b = 3$, and $c = 1$. The red, green, and blue nodes on the outside face of the hexagon graph are connected such that no two nodes of the same color are endpoints of the same path.

there is a relation between the moveable boxes in a double-box configuration η and the closed loops in the corresponding tripartite double-dimer configuration π , thus giving a relation between $\chi(\eta)$, as given by [Definition 5](#), and $2^{\ell(\pi)}$ where $\ell(\pi)$ is the number of closed loops of π . Details of this relation are omitted here due to space constraints.

We now make the following definition:

Definition 6. Let $DDC(\sigma_{a,b,c})$ be the set of all double-dimer configurations on the infinite hexagon lattice such that for each $\pi \in DDC(\sigma_{a,b,c})$, there exists $N \in \mathbb{N}$ such that π restricted to $H(N)$ has the tripartite node pairing $\sigma_{a,b,c}$.

For elements of $DDC(\sigma_{a,b,c})$, we define the generating function as

$$Z_{DDC}^{a,b,c}(q) := \lim_{n \rightarrow \infty} Z_{DDC}^{n;a,b,c}(q) = \frac{1}{w(\pi_0)} \sum_{\pi \in DDC(\sigma_{a,b,c})} 2^{\ell(\pi)} w(\pi). \quad (2.4)$$

Proof that $Z_{DDC}^{a,b,c}(q)$ is well-defined is omitted here due to space constraints.

3 Mapping double-box to double-dimer

Our first main result is the following:

Theorem 2. *Let $a, b, c \in \mathbb{N}$. Then*

$$Z_{\text{DBC}}^{a,b,c}(q) = Z_{\text{DDC}}^{a,b,c}(q) \quad (3.1)$$

where $Z_{\text{DBC}}^{a,b,c}(q)$ is the generating function for double-box configurations as defined in Equation 2.2, and $Z_{\text{DDC}}^{a,b,c}(q)$ is the generating function for double-dimer configurations on the hexagon lattice with tripartite node pairing $\sigma_{a,b,c}$ as defined in Equation 2.4.

The mapping between double-box configurations and double-dimer configurations is easy to visualize via the folklore bijection, but significantly more difficult to prove. To visualize, we apply the folklore bijection (see Figure 1) to the double-box configurations. The result is a triple-dimer configuration on the hexagon graph, which is composed of a single-dimer configuration for each plane partition of $\eta = (\eta_1, \eta_2, \eta_3)$, overlayed such that the point (a, b, c) in \mathbb{R}^3 is the center hexagon (see Figure 7). We show that removing the single-dimer configuration corresponding to the plane partition η_{int} results in a double-dimer configuration on the hexagon lattice with the tripartite node pairing $\sigma_{a,b,c}$.

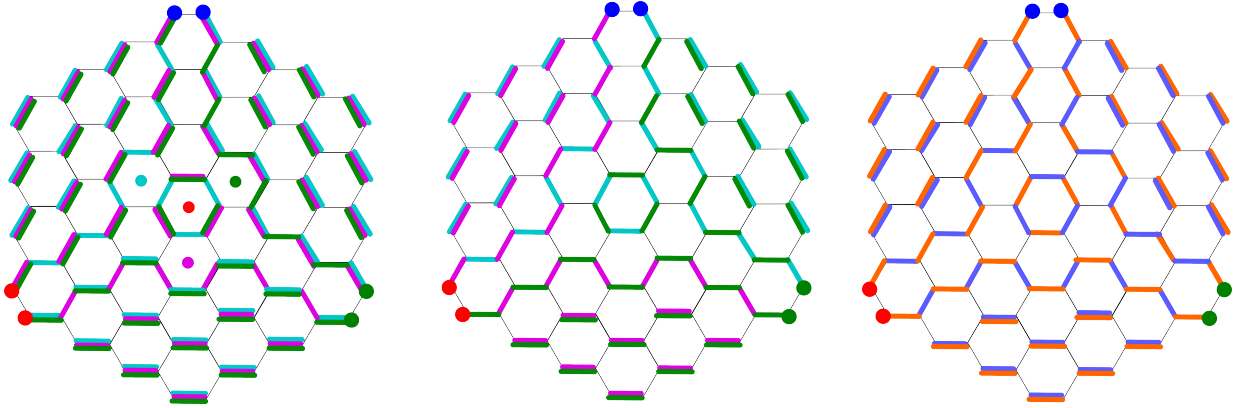


Figure 7: The tripartite double-dimer configuration corresponding to $\eta = (\eta_1, \eta_2, \eta_3)$ from Figure 4. On the left, we have the three single-dimer configurations from η_1, η_2 and η_3 overlayed, with the projected basepoints of η_1, η_2 and η_3 in green, blue, and pink (compare to Figure 3). The middle figure is the double-dimer configuration obtained after removing the single-dimer configuration corresponding to η_{int} (note that triple edges become double edges, and double edges become single edges). On the right is the same double-dimer configuration with different colors to emphasize that the result is in fact a tripartite double-dimer configuration.

To prove [Theorem 2](#), we map the double-box configurations to the tripartite double-dimer configurations via a composition of several maps. We first define a map from the double-box configurations to pairs of objects (π_1, π_2) , where π_1 is an order ideal under the product order on $\mathbb{Z}_{\geq 0}^3$ (i.e. a plane partition) and π_2 is an order ideal under the product order on $\mathbb{Z}_{\geq 0}^3$ which contains M , where M is defined as the infinite collection of boxes

$$M = ([0, a] \times [0, b] \times \mathbb{Z}_{\geq 0}) \cup (\mathbb{Z}_{\geq 0} \times [0, b] \times [0, c]) \cup ([0, a] \times \mathbb{Z}_{\geq 0} \times [0, c]).$$

We then define a map which takes pairs of these objects (π_1, π_2) to another plane-partition-like object called an AB configuration, which comes from Pandharipande–Thomas (PT) theory. AB configurations are defined by Jenne, Webb, and Young in [4] as the discrete version of the labelled box configurations defined by Pandharipande and Thomas in [7]. We then use the work of Jenne, Webb, and Young in [4] to map the AB configurations to the tripartite double-dimer configurations. Using these maps, we show that double-box configurations map to objects (π_1, π_2) which satisfy a labeling algorithm on the boxes, and that these labelled pairs (π_1, π_2) correspond to double-dimer configurations on the hexagon graph with the tripartite node pairing $\sigma_{a,b,c}$ as defined in [Section 2.2](#). The difficulty in proving the equivalence of generating functions of these objects lies in the fact that these maps are not one-to-one.

4 Condensation

Once we have the equivalence of generating functions given by [Theorem 2](#), we may operate in the land of double-dimer configurations, which offers us many tools we can use to prove [Theorem 1](#). We show that both sides of Equation 1.1 satisfy a quadratic recurrence called *condensation*, with the same initial conditions.

On the right hand side of Equation 1.1, we have $M(q)^2 M_{a,b,c}(q)$, which we will denote by $X(a, b, c)$. We show that $X(a, b, c)$ satisfies the following recurrence relation

$$\begin{aligned} X(a, b, c)X(a+1, b+1, c) &= q^c X(a+1, b, c)X(a, b+1, c) \\ &\quad + X(a+1, b+1, c-1)X(a, b, c+1). \end{aligned}$$

Note that $M(q)^4$ factors out of every term, and so we want to show that

$$M_{a,b,c}(a)M_{a+1,b+1,c}(q) = q^c M_{a+1,b,c}(q)M_{a,b+1,c}(q) + M_{a+1,b+1,c-1}(q)M_{a,b,c+1}(q).$$

This follows from Kuo’s graphical condensation (Theorem 6.2 in [6]), where c is the height of the room, with a small modification made which puts the factor of q^c on the

first term instead of the second term as in Theorem 6.2 in [6] (this modification relates to how we overlap the graph sections to obtain the recurrence, details are omitted here).

For the left hand side of Equation 1.1, we may consider $Z_{DDC}^{a,b,c}(q)$ instead of $Z_{DBC}^{a,b,c}(q)$ by Theorem 2. We apply *double-dimer condensation*, a result of Jenne [3], to $Z_{DDC}^{n,a,b,c}(q)$, which we denote here by $Z_{DDC}^n(a,b,c)$ to emphasize the change in a,b,c in the recurrence. This gives the following relation

$$Z_{DDC}^n(a,b,c)Z_{DDC}^n(a+1,b+1,c) = Z_{DDC}^n(a,b+1,c)Z_{DDC}^n(a+1,b,c) \\ + q^K Z_{DDC}^{n,down}(a+1,b+1,c-1)Z_{DDC}^{n,up}(a,b,c+1). \quad (4.1)$$

We calculate this constant K , and show that it does not depend on n . Thus the limit is well-defined, and so $Z_{DDC}^{a,b,c}(q)$ also satisfies this recurrence. Lastly, we show that both sides satisfy the same initial conditions. Details are omitted here, due to space constraints.

Acknowledgements

We would like to thank Amin Gholampour and Martijn Kool for helpful conversations, as well as Cruz Godar and Ava Bamforth. Some illustrations in this paper were created with Dimerpaint, written by Leigh Foster and the second author.

References

- [1] A. Gholampour and M. Kool. “Rank 2 wall-crossing and the Serre correspondence”. *Selecta Math. (N.S.)* **23.2** (2017), pp. 1599–1617. [DOI](#).
- [2] A. Gholampour, M. Kool, and B. Young. “Rank 2 sheaves on toric 3-folds: classical and virtual counts”. *Int. Math. Res. Not. IMRN* **10** (2018), pp. 2981–3069. [DOI](#).
- [3] H. Jenne. “Combinatorics of the double-dimer model”. *Adv. Math.* **392** (2021), Paper No. 107952, 85 pp. [DOI](#).
- [4] H. Jenne, G. Webb, and B. Young. “The combinatorial PT-DT correspondence”. 2020. [arXiv: 2012.08484](#).
- [5] R. W. Kenyon and D. B. Wilson. “Combinatorics of tripartite boundary connections for trees and dimers”. *Electron. J. Combin.* **16.1** (2009), Research Paper 112, 28 pp. [DOI](#).
- [6] E. H. Kuo. “Applications of graphical condensation for enumerating matchings and tilings”. *Theoret. Comput. Sci.* **319.1-3** (2004), pp. 29–57. [DOI](#).
- [7] R. Pandharipande and R. P. Thomas. “The 3-fold vertex via stable pairs”. *Geom. Topol.* **13.4** (2009), pp. 1835–1876. [DOI](#).